EAN 2024 62th annual conference on experimental stress analysis

Prediction of fatigue life of 42CrMo4+QT steel using self-heating effect

Martin Matušů [1,2, a], Jan Papuga [1]

[1]*Department of Mechanics, Biomechanics and Mechatronics, Faculty of Mechanical Engineering, Czech Technical University in Prague, Technická 4, 160 00, Prague, Czech Republic*

[2] *Department of Mechanical and Environmental Engineering, OTH Amberg-Weiden, Germany*

[a]*martin.matusu@fs.cvut.cz*

Abstract: This study proposes a novel approach that takes advantage of the self-heating effect during cyclic loading, showing promise for the prediction of fatigue life. The self-heating phenomenon offers valuable insight into material behaviour, but the stabilised temperature increase used as the key parameter might be absent in some cases. Introducing a modified version of Fargione's method, the study addresses such scenarios in the temperature response of specimens from 42CrMo4+QT steel examined here. Experimental investigations on five datasets, each with different machining parameters, analyse how they influence fatigue life and residual stresses. The findings indicate that the proposed approach could also be applied to materials lacking temperature increase. Challenges related to variable-limiting energy are explored, along with proposed solutions for future evaluation. In summary, this study introduces a promising path to assess fatigue life in materials with an unconventional temperature response during cyclic loading.

Keywords: Fargione's method, self-heating effect, 42CrMo4, fatigue life, surface quality

Nomenclature:

a_1, a_2	[K·MPa^{-1}], [-]	Coefficients for fitting the relation between σ_a and Φ
N_{1-2}	[-]	Number of cycles before transition to second phase
N_f	[-]	Number of cycles to failure
NETD	[mK]	Noise Equivalent Temperature Difference
Φ	[K]	Limiting energy
Φ_0	[K]	Limiting energy related to first phase
Φ_1	[K]	Limiting energy related to linear evolution in second phase
Φ_c	[K]	Limiting energy related to constant temperature delta in second phase
Φ_f	[K]	Limiting energy related to the last phase before break
R	[-]	Load ratio (minimum to maximum load)
R_a, R_z	[µm]	Mean arithmetic roughness, Maximum peak to valley height roughness
R_o	[K·s^{-1}]	Initial temperature rate
R_1	[K·s^{-1}]	Temperature rate in the second phase of temperature evolution
R_y	[K·s^{-1}]	Temperature rate at the last phase before break
SH		Self-Heating
σ_a	[MPa]	Stress amplitude
σ_{FL}, *FL*	[MPa]	Fatigue limit
T_{abs}	[K]	Absolute ambient temperature
T_{loaded}	[K]	Temperature of a dynamically loaded specimen
$T_{reference}$	[K]	Temperature of a reference specimen
Θ	[K]	Stabilized temperature increase

1 Introduction

Materials may fail under cyclic loading even when the load amplitude does not reach the tensile or yield strengths. The S-N (Stress-Life) curve is formed for the specific levels of the stress (S) cycles, which are repeated for some obtained numbers (N) of cycles till break. Predicting cycles to failure is crucial in engineering applications [1]. However, traditional methods for assessing experimental fatigue life are costly and time-consuming due to equipment requirements and the need for testing numerous specimens over many cycles to establish the S-N curve. Standard guidelines [2] suggest the use of 6-12 samples for research purposes

and 12-24 specimens for structural component design. Reducing the number of samples while maintaining the accuracy of the S-N curve would yield significant cost and time savings.

The fatigue life prediction methods discussed here are based on measuring the surface temperatures of a specimen, which fluctuate during cyclic loading. This fluctuation is often monitored using an infrared camera. The difference between the ambient temperature and the surface temperature of the loaded sample is an outcome of cyclic loading, which correlates with intrinsic damage and the response of the structure to loading. This phenomenon is referred to as the Self-Heating (S-H) effect. This approach has demonstrated promising results in both steel specimens [3; 4] and aluminium specimens [5; 6].

The S-H phenomenon relates to the heating of a sample during cyclic loading, where stress amplitudes induce plastic deformations classified as damaging and non-damaging [7]. By mapping material response based on surface temperature, we can effectively analyse fatigue behaviour, including the determination of theoretical fatigue limits [8]. The self-heating effect is inherent in the response of the material to cyclic loading [9; 4]. During repeated loading at a constant amplitude, the temperature monitored on the specimen surface typically exhibits three distinct phases illustrated in Fig. 1, each characterised by specific parameters.

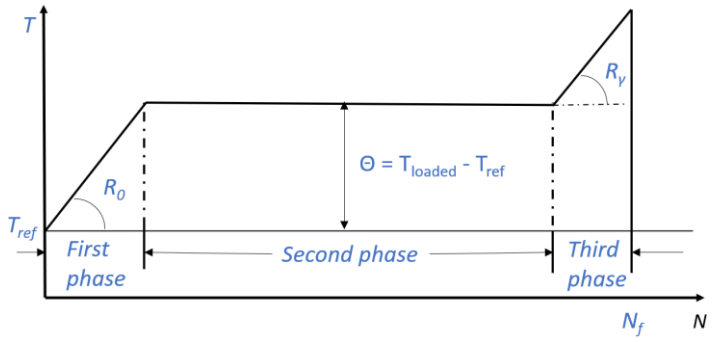

Fig. 1 Schematic depiction of three different phases in temperature response during constant-amplitude cyclic loading until failure at N_f number of cycles.

The initial phase (Phase 1) of the temperature evolution during cyclic loading at a constant load amplitude is marked by a rapid temperature increase. This phase is characterised by the variable R_0, representing the temperature derivative with respect to the number of cycles. The use of this rate to predict fatigue life was previously demonstrated in a study of reversed bending [10].

Phase 2 is of significant importance in this study, representing the constant temperature Θ response of the sample throughout most of its lifespan. This phase is characterised by a steady state, where input work in the system is equally dissipated into the surrounding environment. This parameter is crucial for many works, as seen in the references [11; 12].

The final phase is marked by a rapid increase in temperature that occurs briefly during crack growth before the sample reaches its breaking point. This phase can be effectively delineated by R_y rate, representing the temperature derivative with respect to the number of cycles or time.

The presence and duration of the Phase 2 interval are intricately linked to both the load amplitude and the resulting heat generation within the material. In some cases, Phase 2 may be entirely absent, observed when the load amplitude reaches such high levels that the transition from Phase 1 bypasses Phase 2 entirely, progressing directly to Phase 3, and culminating in the eventual fracture of the specimen.

These three characteristic phases of temperature evolution are commonly observed in metallic structures, mainly analysed for steel alloys [13; 14; 3; 4; 15; 16], due to the presence of a theoretical fatigue limit. Similarly, for aluminium alloys [17], fatigue limit transitions are present.

An alternative response to cyclic loading is observed in certain materials, such as pure copper [18]. While these materials also exhibit a temperature evolution separated into three phases, Phase 2 deviates from the constant temperature response seen in other materials. Instead, the temperature in Phase 2 fails to stabilise, and a non-zero temperature increase rate becomes apparent (see Fig. 2.). This unique behaviour adds an additional layer of complexity to the cyclic loading responses, showcasing the diverse nature of the material responses under different loading conditions.

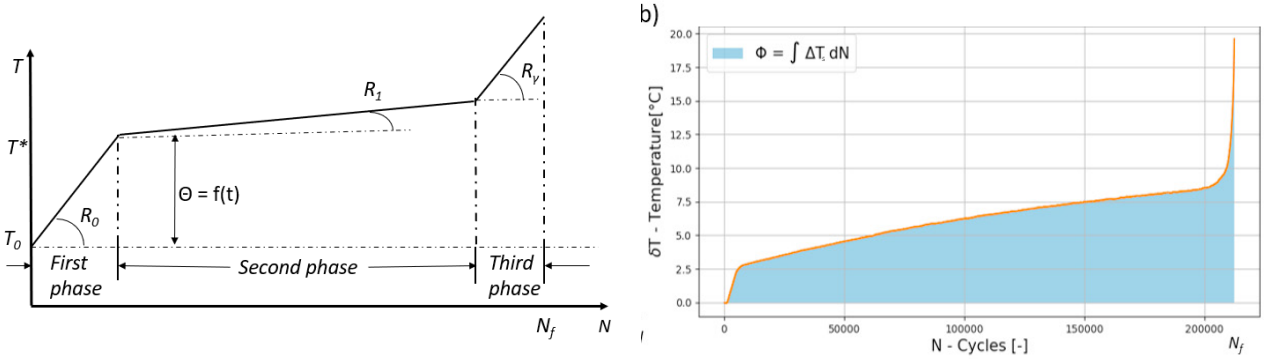

Fig. 2 Schematic representation of three phases of the temperature response during constant-amplitude cyclic loading until N_f at failure, but without any stabilised region in Phase 2.

This paper introduces a modified approach to the prediction of fatigue life, based on Fargione's method [3], with a specific emphasis on the self-heating effect. In particular, our study addresses cases where the temperature evolution lacks Phase 2, as observed in previous research [19]. Five configurations of conventionally manufactured steel were investigated, each with varying surface finishes, leading to various fatigue life performances.

2 Experimental Campaign

This experimental campaign focused on investigating the impact of various machining parameters on the fatigue life performance of the test series A25-29. These series were produced from conventionally manufactured steel 42CrMo4+QT, originating from a single heat source and fabricated from a 35mm diameter bar. Part of a larger campaign conducted throughout Europe, this study builds on previous research exploring the effect of size [20; 21] and self-heating [19]. The ultimate tensile strength and yield stress of the material were determined to be 1097 MPa and 1001.5MPa, respectively. Variations in surface roughness across series A25-A29, influenced by machining parameters used for the finishing cut detailed in the Tab. 1, resulted in different fatigue strengths and thermal responses during fatigue testing. In particular, differences in the final finish were characterized by the roughness achieved and residual stresses on the surface (see Fig. 4). All series were manufactured using the same lathe, with the fatigue specimen geometry depicted in Fig. 3 for all series A25-A29 made from 42CrMo4+QT steel.

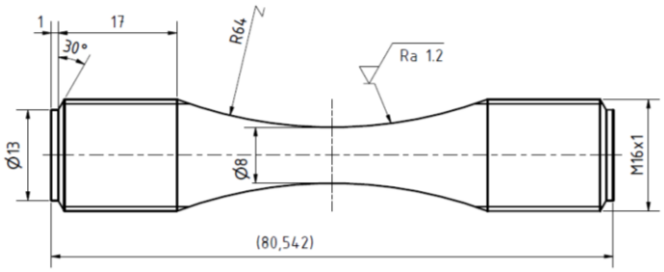

Fig. 3 Geometry of fatigue specimens manufactured from 42CrMo4+QT steel, within the project [22; 23; 19].

All fatigue experiments were conducted on an Amsler resonant (see Fig. 5) pulsator at CTU in Prague with a load ratio of R = -1 and testing frequency of around 150Hz. This difference in fatigue performance of each series is attributed to the variation of production parameters, leading to high residual stresses on the surface of the specimens (see Table 1, and the legend of the graph in Fig. 4), particularly noticeable in tension for all series as so as the roughness of final finish. In particular, A28 shows the poorest fatigue performance, despite a similar S-N curve trend ranging from 10^4 to 10^5 for both A28 and A26. Series A27 and A25 exhibit nearly identical fatigue curve regressions using the K&V regression method [24]. Furthermore, the K&V regression of A29 and A26 demonstrates a nearly identical transition to the fatigue limit domain. The lower fatigue

performance of A28 could also be attributed to the highest measured roughness (see Tab. 1). The fatigue limit was established as an asymptote to the K&V regression [24].

In this paper, the focus is set on self-heating and fatigue life estimation derived from the self-heating effect. Consequently, the detailed description of the fatigue strength corresponding to various machining parameters is described in another publication by Papuga et al. [25].

Tab. 1: Different turning parameters used for machining the fatigue samples for series A25-A29. All series were turned without additional grinding or polishing.

		A25	A26	A27	A28	A29
Cutting speed at D=8mm	V_c [m/min]	75	75.4	100	62.8	75.4
Feed rate	F [mm/rev]	0.05	0.05	0.1	0.1	0.1
Process fluid (Decocut 1040 during roughing)	Y/N	Y	Y	Y	Y	Y
Cooling fluid during last cuts	Y/N	Y	N	Y	N	N
Cutter nose radius	R [mm]	0.4	0.4	0.4	0.4	0.4
Last cut height	[mm]	0.05	0.1	0.1	0.05	0.1
Second-last cut height	[mm]	0.1	0.1	0.1	0.1	0.1
Third-last cut height	[mm]	0.15	0.1	0.1	0.15	0.1
Ra	[µm]	1.26	0.67	1.2	1.46	0.87
Rz	[µm]	6.4	3	5.4	7.1	3.3

Self-heating experiments were performed using thermal camera Flir A315 (with the *NETD* of 50mK) with surface of the samples covered with high emissivity painting from LabIR (HERP-LT-MWIR-BK-11) to improve the precision of the measurement. Near the loaded specimen, a reference non-loaded specimen was positioned. Serving as a stable temperature reference, this unloaded sample played a crucial role in our measurements. When the thermal differentials between the loaded and unloaded samples were compared, the heat generation within the loaded specimen could be assessed more accurately.

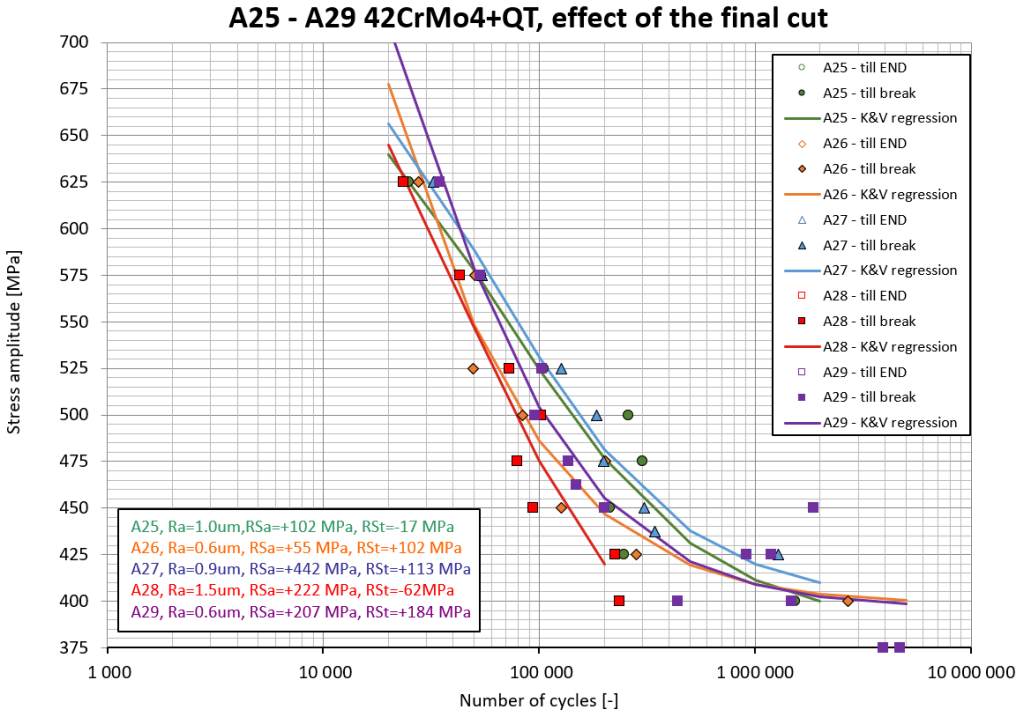

Fig. 4 Fatigue life curves with K&V regression for A25-A29. The *RSa* parameter refers to the residual stress in the axial direction, and *RSt* is the residual stress in the tangential direction.

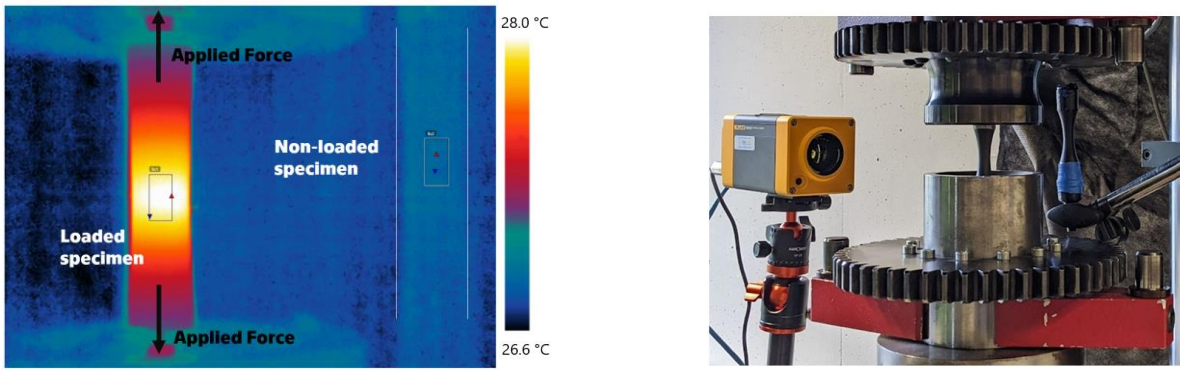

Fig. 5 Thermal image (FLIR A315 320×240p, with frame rate 3.75 Hz) of the reference specimens and loaded (left). Amsler resonant pulsator with a FLUKE RSE600 thermal imaging camera. The loaded and reference specimens are installed in the machine (right).

3 The Fargione method

The method proposed by Fargione [3], also utilized by Lipski [26], offers an intriguing analysis of the relationship between applied stress and the number of cycles to failure. Central to this method is the concept of "limiting energy“ derived from the second law of thermodynamics. This principle states that a body can generate only a certain amount of entropy before structural failure occurs, essentially representing the maximum disorderliness achievable. Fargione defines this energy as the integration of the temperature evolution curve over the interval of cycles from the start of the measurement to the point of failure. He suggests that Phases 1 and 3 are negligible, leading to the definition of an area as a function of the number of cycles to failure and the stabilised temperature increase, Eq. (1). This concept is sometimes referred to as "finite energy" or "limiting energy," representing a parameter associated with the finite entropy of the system; see Fig. 6.

$$\Phi = \int_0^{N_f} T(N)\, dN = const. \tag{1}$$

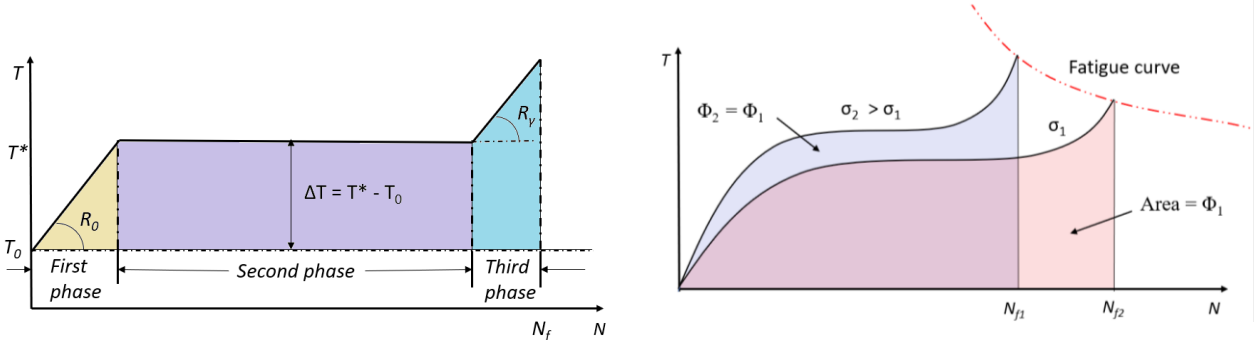

Fig. 6 The figure on the left represents the expected temperature evolution for the use of the Fargione method. The right scheme illustrates Fargione’s method with estimating the number of cycles to failure for each amplitude of load with the use of the concept of the limiting energy.

Fargione's approach [3] expands into thermographic analysis, providing deeper insight into material behaviour under cyclic loads compared to Risitano's method [14]. The goal is not only to determine the fatigue limit, but also to characterise the entire S-N curve. Component failure under dynamic loads is attributed to microplasticity, leading to increased yielding. In this context, a limiting energy is introduced to describe the dissipated energy throughout the failure process. The heat energy which is directly proportional to the limiting energy Φ can be interpreted as the integral of the $\Theta(N)$ function. Fargione postulates that this limiting energy remains constant, serving as a characteristic for the material or component.

Rearranging the formula, the number of cycles until fracture (N_f) can be determined from the observed stabilised temperature increase Θ. Since Θ is characteristic of the applied stress amplitude according to Risitano [14], N_f can be correlated with the stress amplitude σ_a through this relationship. The characteristic stabilised temperatures are obtained from the step test (see Fig. 7), allowing the numbers of cycles N_f to be associated with every corresponding stress amplitude σ_a. This method requires a step test for multiple stress levels and, optionally, a pure $\Theta(N)$ curve from the onset to the failure (single-level test). The stress amplitude should be well above the fatigue limit to determine the limiting energy of the single-level test, ensuring that the test is ended by a failure of the specimen. While theoretically achievable with a single sample, at least three samples are recommended for calculating an average value of limiting energy, as well as for the S-H step-test.

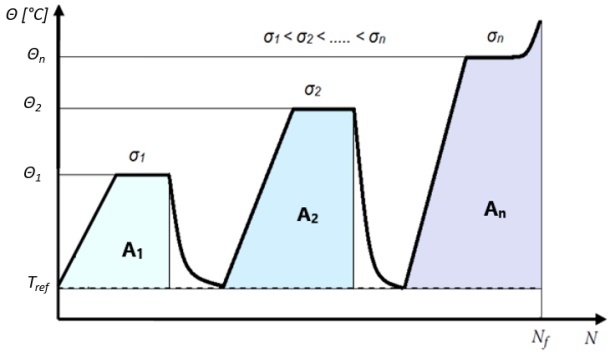

Fig. 7 Scheme of the Self-Heating (S-H) step test with the step amplitudes subsequently increasing in each step and depicted limiting energy areas A_i within each loading block.

As Eq. (1) relies on the entire temperature evolution, it needs to be simplified. Our goal is to identify a measurable parameter, specifically the stabilised temperature in Phase 2, that can be consistently monitored across sequential loadings on a single sample during the self-heating step-test. Fargione recommends using the 1st and 2nd phases, as stated in Eq. (2)

$$\Phi \approx \frac{1}{2} \cdot \Theta \cdot N_{1-2} + \Theta \cdot \left(N_f - N_{1-2}\right) = const. \quad (2)$$

where the stabilised temperature Θ represents the temperature increase in Phase 2, denoted by Θ. The value of $N_{1\text{-}2}$ corresponds to the number of cycles at the transition from Phase 1 to Phase 2. Phase 3 is ignored, as it cannot be accounted for in the SH step test with a variable amplitude. To simplify Eq. (2), Phase 1 is neglected, as it plays a minor role in the limiting energy parameter, as stated in [3] in certain cases. Fargione's limiting energy parameter is then simplified to:

$$\Phi \approx \Theta \cdot N_f = const. \quad (3)$$

3.1 Modification of the Fargione method for special cases of 42CrMo4+QT

In this section, an improved version of Fargione's method was developed to address the non-standard thermal response observed in special cases. The same batch of 42CrMo4+QT was examined in other articles [19; 23; 27]. However, the primary focus here is on the S-H effect, with reference [19] highlighting a critical issue: the absence of the stabilised temperature increase in Phase 2, as illustrated in Fig. 2. For this paper, the fatigue limit (FL) is defined as the value obtained as an asymptote to the K&V regression [24], mainly because most FL estimation methods rely on temperature stabilisation in the second phase. Despite testing various parameters of the temperature evolution, no results directly related to FL were obtained [19].

Determining the limiting energy typically involves cyclically loading a single specimen at a specific stress amplitude until failure occurs. If Fargione's assumption, as expressed in Eq.(1), holds true, this limiting energy value can be utilised to estimate the number of cycles to failure at other stress levels, provided that the stabilised temperature response to the corresponding load amplitudes is acquired. It is crucial to acknowledge that relying solely on a single limiting energy value can be misleading, as it disregards the statistical nature of fatigue damage, which follows a distribution rather than a precise value.

An intriguing application of Fargione's theory, as outlined in Eq. (1), involves the experimental determination of the S-N curve using only two test specimens. One specimen is utilised to obtain the limiting energy value, while the second specimen undergoes testing with progressively increasing stress amplitudes, as depicted in Fig. 6 (right). In the specific cases addressed here, up to nine samples from constant-amplitude tests intended to determine the S-N curve were utilized to calculate the limiting energy. This approach allows for a deeper understanding of whether the limiting energy remains constant or varies with the stress amplitude.

In the case of the 42CrMo4 + QT tests described earlier; it was observed that there is no section of the stabilised temperature increase [19]. Another assumption had to be made because the Fargione method is based on reaching the stabilised Phase 2. This acknowledges the dynamic nature of the testing process and aims to incorporate any initial changes and subsequent stabilisation in Phase 2, ensuring a more accurate estimation of fatigue behaviour.

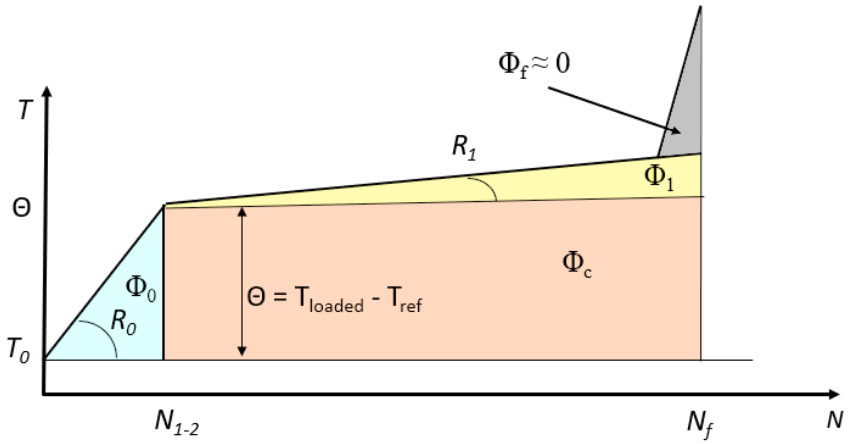

Fig. 8 Four segments of the limiting energy. The sum of all partial limiting energies represents the limiting energy of the whole temperature evolution.

Fig. 8 presents a schematic representation that illustrates the separation of the limiting energy into four distinct areas of focus. Each of these areas contributes to the overall limiting energy of the entire temperature evolution. By considering the cumulative sum of these four areas, the limiting energy can be obtained. To implement the Self-Heating step-test with variable load amplitude, which comprises only Phase 1 and Phase 2 of temperature evolution during cyclic loading, the segmentation assumes a linear behaviour in the second phase. This approach allows for the estimation of the limiting energy for the entire temperature evolution based on a small segment of the total lifespan, thereby predicting the number of cycles to failure.

The main change involves setting the limiting energy from the measured parameters of the Θ -N record obtained from a step test, using the $N_{1\text{-}2}$ which is the number of cycles at the end of the first phase, the secondary temperature increase rate in Phase 2 R_1 and the temperature Θ which is related to the original Fargione method described in Fig. 2. In this paper, limiting energy is assumed to be a function of the load amplitude as observed by Lipski [26] or in [19; 5]. To demonstrate the relationship between stress amplitude and failure limits of the tested specimens at a single level, see Fig. 9. It is evident that as stress amplitude increases, the limiting energy decreases, highlighting the variable nature of this parameter in this specific scenario.

The area most related to the original Fargione's assumption Eq. (3) is Φ_c (referred to as c as its main parameter is stabilized temperature Θ) that can be described as:

$$\Phi_c \approx \Theta(N_f - N_{1-2}), \tag{4}$$

where Φ_c represents a part of the limiting energy as depicted in Fig. 8. $N_{1\text{-}2}$ represents the length of Phase 1 in cycles, and it is set as an intersection of the record segments with rates of R_0 and R_1. Another segment is the area in Phase 1 described as Φ_0:

$$\Phi_0 \approx \frac{1}{2}\Theta N_{1-2}, \tag{5}$$

The main reason for the modification of Fargione's original approach is the R_1 rate in Phase 2, which creates a new partial limiting energy segment Φ_1:

$$\Phi_1 \approx \frac{1}{2}\tan R_1 \left(N_f - N_{1-2}\right)^2. \quad (6)$$

Eq. (6) can be further simplified so that the tangent of an angle, which is nearly zero, is equal to the angle itself. Since Phase 3 does not occur in the self-heating step test with a variable load amplitude, the partial limiting energy Φ_f (f as an area close to failure of the structure) is neglected in this model, but it is supposed to be nearly equal to zero. Using the Eq. (4) to (6), the limiting energy of the entire test is then described as follows:

$$\Phi \approx \Theta\left(N_f - N_{1-2}\right) + \frac{1}{2}\Theta \cdot N_{1-2} + \frac{1}{2}\tan R_1 \left(N_f - N_{1-2}\right)^2. \quad (7)$$

It is also assumed that the limiting energy is not constant across various stress amplitudes, but that it is constant for the same stress amplitude in the same testing condition and for the same material. It is assumed that the function of the limiting energy to the stress amplitude is a power-law function:

$$\Phi \approx f(\sigma_a), \Phi \approx a_1 {\sigma_a}^{a_2}. \quad (8)$$

Coefficients a_1 and a_2 in Eq. (8) are determined experimentally from single-level tests to failure of the specimen. For the series used in this experiment campaign, A25-A29, the coefficients are established using regression, as shown in the Tab. 2. It is worth noting that the coefficients of determination are relatively low, primarily due to the scatter of data, as depicted in Fig. 9.

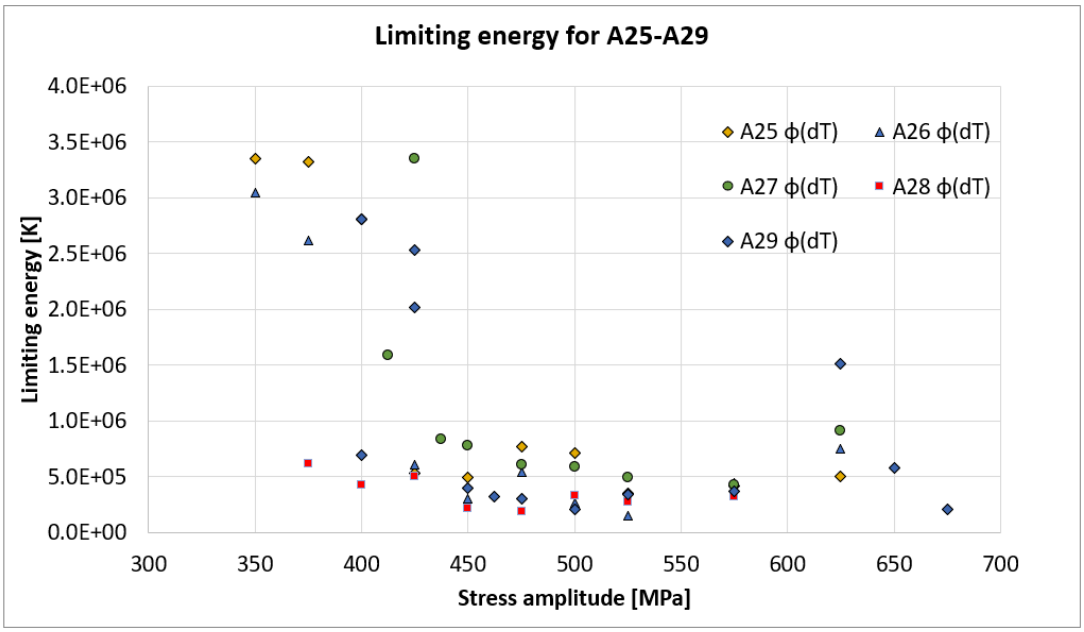

Fig. 9 Relation between stress amplitude and limiting energy calculated according to single level test for series A25-A29.

Tab. 2: Coefficients for describing the limiting energy via the power-law function Eq. (8).

	a_1	a_2	R^2
A25	2.93E+16	-3.95	0.81
A26	9.90E+16	-4.17	0.48
A27	9.02E+06	0.00	0.31
A28	8.60E+09	-1.66	0.52
A29	8.92E+16	-4.09	0.53

The number of cycles is then set as follows using Eq. (7) and (8):

$$N_f \approx \frac{1}{2}\left(\left(2N_{1-2} - \frac{\Theta}{2R_1}\right) + \sqrt{\left(-2N_{1-2} + \frac{\Theta}{2R_1}\right)^2 - 4\cdot\left(N_{1-2}^2 - \frac{\Theta N_{1-2}}{4R_1} - \frac{\left(\frac{\sigma_a}{a_1}\right)^{1/a_2}}{2R_1}\right)}\right) \quad (9)$$

3.2 Application of the modified Fargione method

First, the limiting energy is calculated, and the coefficients of the power law Eq. (8) are established as outlined in the Tab. 2. Subsequently, using Eq. (9), the number of cycles is determined for each stress amplitude in the S-H step test. This calculation requires input parameters such as $N_{1\text{-}2}$, R_1,Θ (obtained from the self-heating step test) and σ_a from the load cell of the Amsler resonant pulsator.

The self-heating step test was performed to determine $N_{1\text{-}2}$, R_1, and Θ, with a focus on stress amplitudes well below the fatigue limit for each configuration. The test block comprised 15,000 cycles per stress amplitude, with the stress amplitudes progressively increasing until failure. The primary objective was to estimate the S-N curve, when the conventional Fargione approach using stabilized temperature was not applicable. In the absence of a lower limit of usability of Fargione's method, it is assumed that the fatigue limit is the lower boundary [28]. In this study, the fatigue limit is determined from the data obtained from the experimentally derived S-N curve (refer to Fig. 4). Each fatigue curve estimation utilised a single sample, except for A29, where three samples could be used thanks to the bigger number of specimens available.

In Fig. 10, the results of the modified Fargione method show a strong correlation with the K&V regression of series A26, A27, and A29, with A29 and A26 exhibiting particularly accurate predictions for the estimated number of cycles to failure. However, without establishing a fatigue limit (FL) as an asymptote to K&V regression [24], this estimate could extend to the lowest value tested, underscoring the need for limitations, which were not identified in this study. Series A28 shows significantly higher fatigue life predictions compared to the experimentally established slope of the S-N curve, suggesting potential inaccuracies in component production. Series A25 shows good correspondence in the upper part of the S-N curve up to $2\cdot10^5$ cycles, with trends nearly identical to A27 but with closer alignment to the experimentally measured S-N curve. However, beyond this point, the trend takes a steeper slope than the measured S-N curve, potentially influenced by an outlier specimen, as observed in the A28 series. The coefficient of determination (R^2) for the A25-A29 series estimates ranges from 0.30 to 0.78, with the lowest R^2 observed for series A28, as discussed earlier.

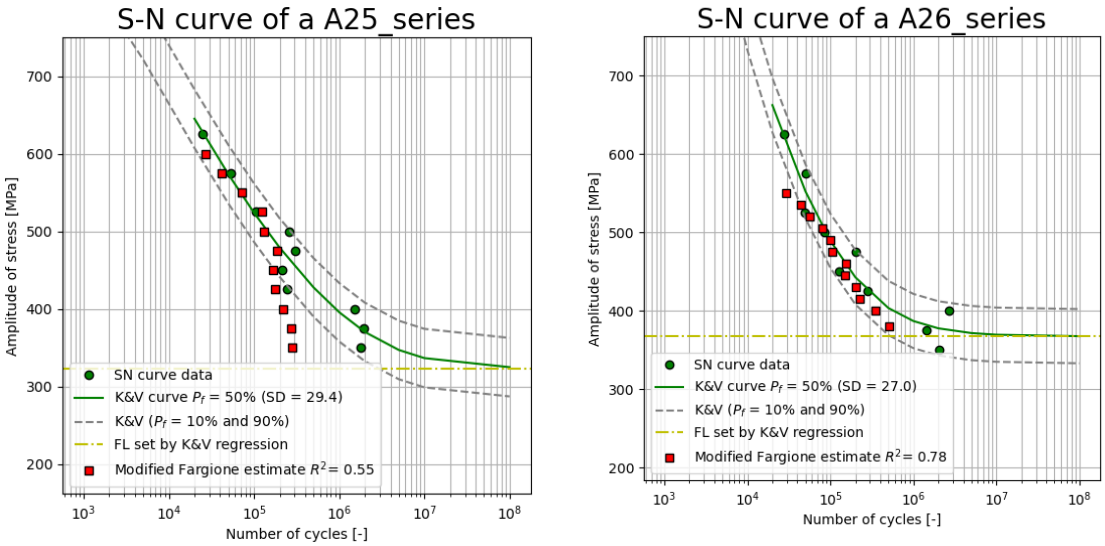

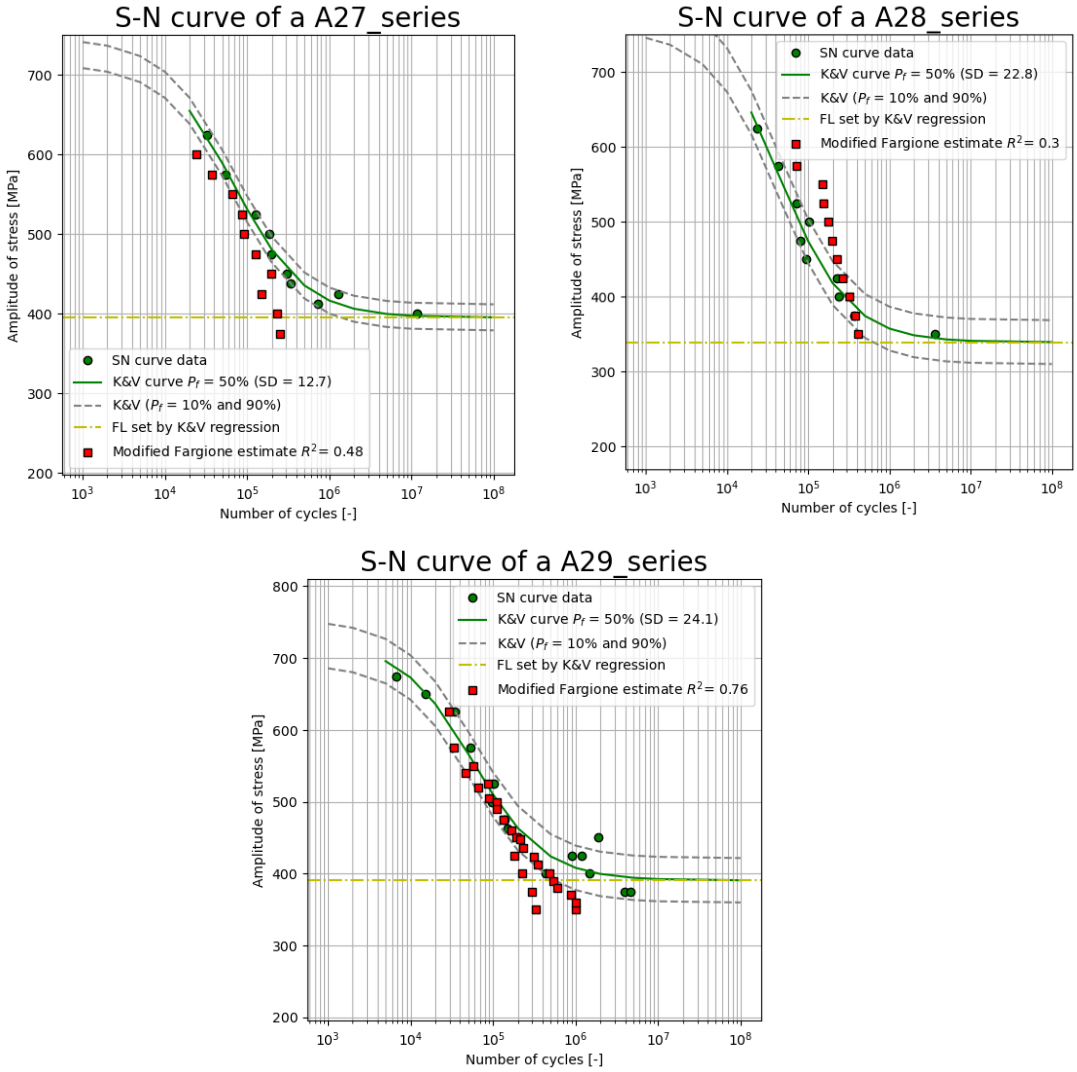

Fig. 10 Modified Fargione method for series A25-A29 with marked estimates and coefficients of determination in each figure.

Undoubtedly, the main drawback of the modified Fargione method lies in the variable limiting energy, as indicated in Tab. 2. The weak correlation of the limiting energy with different stress amplitudes reveals a poor fit to the dataset, reflected in the low coefficient of determination values. Another challenge in predicting the number of cycles to failure stems from the observed shifts in trends, particularly noticeable in A25 and A27 in the modified Fargione estimation. Although this change could potentially result from damage incurred during previous testing levels, such occurrences should ideally be minimised. On the contrary, the single specimen from the A28 series might represent an outlier on the positive side of the S-N curve, leading to potentially misleading estimates. Addressing these issues is paramount for refining this method for presentation purposes.

4 Conclusion

This study presents a comprehensive investigation of fatigue life assessment, focussing on the unique case of the 42CrMo4+QT material and its unconventional temperature response during cyclic loading. Using the self-heating effect and modifying Fargione's method, a promising approach to predicting fatigue life is proposed. The experimental campaign on five datasets highlights the influence of machining parameters on fatigue life and residual stresses, providing insights into material behaviour, however, the main focus of this paper is not on the influence of machining parameters of 42CrMo4+QT steel.

The results of the thermographic observation indicate that this material lacks the typical stabilisation of the temperature of Phase 2 commonly observed. The proposed modification of the Fargione method addresses the abnormal Phase 2 without temperature stabilization, showing promising results in predicting fatigue life.

However, challenges such as variable limiting energy and shifts in trends pose significant considerations for the accuracy and reliability of the method. The application of the modified Fargione approach works partially for the series, where only one sample was dedicated for S-H step-test A25-A28, leading to more conservative results for A25 and A27. Series A28 has its estimate much higher than the S-N curve, which could potentially be caused by using a specimen, that would be an outlier on the right side of the fatigue curve. For future research, employing at least three specimens for the S-H step-test from which the average thermal and fatigue behaviour is obtained, as demonstrated in the A29 series, appears to be the most promising approach.

Acknowledgement

The authors acknowledge the support by the Grant Agency of the CTU in Prague (SGS23/156/OHK2/3T/12 project) and by the Czech Ministry of Education, Youth and Sports (LUABA22071 project).

References

[1] Fatemi A, Yang L. Cumulative fatigue damage and life prediction theories: a survey of the state of the art for homogeneous materials. International Journal of Fatigue 1998;vol. 20:9-34. https://doi.org/10.1016/S0142-1123(97)00081-9.

[2] Standard Practice for Statistical Analysis of Linear or Linearized Stress-Life (S-N)and Strain-Life (e-N) Fatigue Data 1981.

[3] Fargione G. Rapid determination of the fatigue curve by the thermographic method. International Journal of Fatigue 2001;vol. 24:11-19. https://doi.org/10.1016/S0142-1123(01)00107-4.

[4] Meneghetti G. Analysis of the fatigue strength of a stainless steel based on the energy dissipation. International Journal of Fatigue 2007;vol. 29:81-94. https://doi.org/10.1016/j.ijfatigue.2006.02.043.

[5] Matušů M, Dimke K, Šimota J, Papuga J, Rosenthal J, Mára V, Beránek L. Energy-based method for analyzing fatigue properties of additively manufactured AlSi10Mg. Journal of Mechanical Science and Technology 2023;37:7. https://doi.org/10.1007/s12206-022-2110-6.

[6] Seitl S, Klusák J, Pelayo F, Canteli A. Thermographic Determination Methodology: Application on Fatigue Limit of AL 2024 for R=-1. Key Engineering Materials 2013;577-578:477-480. https://doi.org/10.4028/www.scientific.net/KEM.577-578.477.

[7] Klesnil M, Lukáš P. Fatigue of metallic materials. 3. upr. vyd. Praha: Academia; 1992.

[8] Matušů M, Džuberová L, Papuga J, Rosenthal J, Šimota J, Beránek L. Fatigue analysis and heat treatment comparison of additively manufactured specimens from AlSi10Mg alloy. International Journal of Fatigue 2024;vol. 185:18. https://doi.org/10.1016/j.ijfatigue.2024.108357.

[9] Guo Q, Zaïri F, Yang W. Evaluation of intrinsic dissipation based on self-heating effect in high-cycle metal fatigue. International Journal of Fatigue 2020;vol. 139. https://doi.org/10.1016/j.ijfatigue.2020.105653.

[10] Amiri M, Khonsari M. Rapid determination of fatigue failure based on temperature evolution: Fully reversed bending load. International Journal of Fatigue 2010;vol. 32:382-389. https://doi.org/10.1016/j.ijfatigue.2009.07.015.

[11] Prochazka R, Dzugan J, Konopik P. Fatigue limit evaluation of structure materials based on thermographic analysis. Procedia Structural Integrity 2017;vol. 7:315-320. https://doi.org/10.1016/j.prostr.2017.11.094.

[12] Douellou C, Balandraud X, Duc E, Verquin B, Lefebvre F, Sar F. Fast fatigue characterization by infrared thermography for additive manufacturing. Procedia Structural Integrity 2019;vol. 19:90-100. https://doi.org/10.1016/j.prostr.2019.12.011.

[13] Luong M. Fatigue limit evaluation of metals using an infrared thermographic technique. Mechanics of Materials 1998;vol. 28:155-163. https://doi.org/10.1016/S0167-6636(97)00047-1.

[14] La Rosa G. Thermographic methodology for rapid determination of the fatigue limit of materials and mechanical components. International Journal of Fatigue 2000;vol. 22:65-73. https://doi.org/10.1016/S0142-1123(99)00088-2.

[15] Meneghetti G, Ricotta M. The use of the specific heat loss to analyse the low- and high-cycle fatigue behaviour of plain and notched specimens made of a stainless steel. Engineering Fracture Mechanics 2012;vol. 81:2-16. https://doi.org/10.1016/j.engfracmech.2011.06.010.

[16] Cura F, Curti G, Sesana R. A new iteration method for the thermographic determination of fatigue limit in steels. International Journal of Fatigue 2005;vol. 27:453-459. https://doi.org/10.1016/j.ijfatigue.2003.12.009.

[17] Ezanno A, Doudard C, Calloch S, Millot T, Heuzé J. Fast characterization of high-cycle fatigue properties of a cast copper–aluminum alloy by self-heating measurements under cyclic loadings. Procedia Engineering 2010;vol. 2:967-976. https://doi.org/10.1016/j.proeng.2010.03.105.

[18] Wang X, Crupi V, Jiang C, Feng E, Guglielmino E, Wang C. Energy-based approach for fatigue life prediction of pure copper. International Journal of Fatigue 2017;vol. 104:243-250. https://doi.org/10.1016/j.ijfatigue.2017.07.025.

[19] Matušů M, Papuga J, Mžourek M. Fatigue strength estimation of 42CrMo4 QT from the temperature evolution during cyclic loading. Procedia Structural Integrity 2022;vol. 42:102-109. https://doi.org/10.1016/j.prostr.2022.12.012.

[20] Papuga J, Mžourek M, Matušů M, Mára V, Čapek J. Investigation of the size effect on 42CrMo4 QT steel in the high-cycle fatigue domain part I: Experimental campaign. International Journal of Fatigue 2023;vol. 175. https://doi.org/10.1016/j.ijfatigue.2023.107743.

[21] Mžourek M, Papuga J, Nesládek M, Matušů M, Čapek J, Mára V. Fatigue Damage Analysis On 42CrMo4 QT Via Critical Volume Approach. Procedia Structural Integrity 2022;vol. 42:457-464. https://doi.org/10.1016/j.prostr.2022.12.058.

[22] Mžourek M, Papuga J, Nesládek M, Matušů M, Čapek J, Mára V. Fatigue Damage Analysis On 42CrMo4 QT Via Critical Volume Approach. Procedia Structural Integrity 2022;vol. 42:457-464. https://doi.org/10.1016/j.prostr.2022.12.058.

[23] Papuga J, Mžourek M, Matušů M, Mára V, Čapek J. Investigation of the size effect on 42CrMo4 QT steel in the high-cycle fatigue domain part I: Experimental campaign. International Journal of Fatigue 2023;vol. 175. https://doi.org/10.1016/j.ijfatigue.2023.107743.

[24] Kohout J, Věchet S. A new function for fatigue curves characterization and its multiple merits. International Journal of Fatigue 2001;vol. 23:175-183. https://doi.org/10.1016/S0142-1123(00)00082-7.

[25] Papuga J, Vrbata T, Trojan K, Trefil A, Zabala A, Mára V. The Effect of Specimen Machining Processes on Fatigue Life Of 42CrMo4+Qt Steel. 9th EIS International Conference on Durability & Fatigue – Fatigue 2024 (In - print), Cambridge: Jesus Coledge, UK; 2024, p. 13.

[26] Lipski A. Rapid Determination of the S - N Curve for Steel by means of the Thermographic Method. Advances in Materials Science and Engineering 2016;vol. 2016:1-8. https://doi.org/10.1155/2016/4134021.

[27] Mžourek M, Papuga J, Nesládek M, Matušů M, Čapek J, Mára V. Fatigue Damage Analysis On 42CrMo4 QT Via Critical Volume Approach. Procedia Structural Integrity 2022;vol. 42:457-464. https://doi.org/10.1016/j.prostr.2022.12.058.

[28] Matušů M, Šimota J, Papuga J, Rosenthal J, Reis L, Costa P, Bumba F. Estimation of the S-N curve from limiting energy for additively manufactured specimens from AlSi10Mg. Fatigue & Fracture of Engineering Materials & Structures [Under Review] n.d.:32.